

Heat capacity of high-purity polycrystalline $\text{YBa}_2\text{Cu}_3\text{O}_7$ from 0.4 to 400 K in applied magnetic fields of 0 and 70 kG

W. C. Lee,* K. Sun, L. L. Miller, D. C. Johnston, and R. A. Klemm†
Ames Laboratory-USDOE and Department of Physics, Iowa State University, Ames, Iowa 50011

S. Kim, R. A. Fisher, and N. E. Phillips
Materials and Chemical Sciences Division, Lawrence Berkeley Laboratory, University of California, Berkeley, California 94720
 (Received 16 July 1990)

The heat capacities $C(T)$ of high-purity polycrystalline pellet and powder samples of $\text{YBa}_2\text{Cu}_3\text{O}_7$ are reported for the temperature T in the range 0.4 to 400 K. In addition to the feature associated with the onset of superconductivity at $T_c \approx 91$ K, two clear anomalies in $C(T)$ for the pellet sample were observed near 74 and 330 K; the origins of the latter two anomalies are unknown, but the temperatures at which they occur are similar to those at which anomalies are seen in the temperature-dependent magnetization $M(T)$. The feature in $M(T)$ at ≈ 70 K increases linearly with field H at a rate of 0.30 K/kG for $20 \text{ kG} \leq H \leq 40 \text{ kG}$. The anomaly in $C(T)$ at ≈ 330 K observed for the pellet was not observed for the powder sample, which is consistent with the lack of an anomaly in $M(T)$ near this temperature for the powder sample. For the pellet sample, the electronic entropy near T_c , the contribution of superconducting fluctuations to $C(T)$ near T_c , and the influence of a 70-kG magnetic field on $C(T)$ near T_c and below 10 K are analyzed and discussed. Various features of the $C(T)$ for the pellet sample such as the magnitude of $C(T)$ and the derived Debye temperature and heat capacity jump at T_c , as well as the size and shape of the $C(T)$ anomalies at ≈ 74 and 330 K, were found to depend on the thermal- and/or magnetic-field treatment history of the sample. Differential-thermal-analysis measurements quantitatively determined the BaCuO_2 impurity content in our batch of $\text{YBa}_2\text{Cu}_3\text{O}_7$ to be 0.3(1) wt. %. Coupled with the analysis of the low- T $C(T)$ measurements, we conclude that the linear $C(T)$ coefficient $\gamma(0)$ associated with the $\text{YBa}_2\text{Cu}_3\text{O}_7$ phase in the pellet sample is $\approx 4.0 \text{ mJ/mol K}^2$. It is suggested that some fraction of $\gamma(0)$ could arise from thermal excitation of antiferromagnetic spin waves in the Cu-O chains of the structure.

I. INTRODUCTION

Thermodynamic measurements of the high- T_c cuprate superconductors can yield important information about the normal and superconducting states. The most well studied of these materials is the compound $\text{YBa}_2\text{Cu}_3\text{O}_7$.^{1,2} Measurements of the temperature T dependent anisotropic magnetic susceptibility $\chi(T)$ of high-purity $\text{YBa}_2\text{Cu}_3\text{O}_7$ have revealed that the intrinsic $\chi(T)$ increases monotonically with T from the superconducting transition temperature $T_c \sim 91$ K up to at least 400 K, with negative curvature below ~ 200 K, for applied magnetic fields \mathbf{H} both parallel and perpendicular to the CuO_2 planes of the structure.³ This negative curvature was quantitatively modeled as arising from a combination of superconducting fluctuation diamagnetism and a temperature-dependent normal state $\chi(T)$.^{3,4} From the analysis, microscopic parameters associated with the superconducting state were obtained.

From the above $\chi(T)$ data, the magnetic-phase impurity and Cu^{2+} magnetic-defect levels in the samples from the batch of $\text{YBa}_2\text{Cu}_3\text{O}_7$ measured appeared to be the lowest of any single-crystal or polycrystalline sample for which $\chi(T)$ data had been reported. We concluded that it would be worthwhile to carry out extensive heat-capacity $C(T)$ measurements on this batch, despite the large num-

ber of $C(T)$ studies already reported for this compound.⁵ Our primary goals were to (i) determine whether the nonzero zero-field Sommerfeld coefficients $\gamma(0) \gtrsim 4 \text{ mJ/mol K}^2$ observed in previous low- T $C(T)$ studies⁶ are comparable to or greater than that for our batch and determine whether our observed $\gamma(0)$ is intrinsic⁶ or extrinsic,⁷ (ii) document the influence of superconducting fluctuations on $C(T)$ near T_c ,⁸⁻¹¹ and (iii) ascertain whether the anomalies sometimes observed in $\chi(T)$ measurements near 240 K (Refs. 12 and 13) and/or 320 K,¹² and in other types of measurements at various temperatures, are also manifested in $C(T)$. Herein, we report extensive measurements of $C(T)$ for the above-high-purity batch of $\text{YBa}_2\text{Cu}_3\text{O}_7$ which were carried out in an attempt to address these issues. Complementary magnetization data were obtained and are presented for comparison.

II. EXPERIMENTAL DETAILS

A 15-g master batch of polycrystalline $\text{YBa}_2\text{Cu}_3\text{O}_{7-\delta}$ was prepared from predried 99.99% Y_2O_3 , 99.999% CuO , and 99.9% BaCO_3 . The stoichiometric mixture of starting materials was ground thoroughly in air using an agate mortar and pestle, and fired at 940°C for 1 day in air in an alumina crucible. Then 12 g was pressed into a

$\frac{1}{2}$ -in.-diam pellet, and the remaining 3 g was maintained separately as powder. Both pellet and powder samples were fired at 940°C for 90 days in air with ten intermediate grindings, followed by heating in O₂ at 640°C for 1 day and oven cooling to room temperature. The final pellet sample had a density of 75% of the theoretical value. From powder x-ray-diffraction analysis, the batch of YBa₂Cu₃O_{7- δ} was single phase with lattice parameters $a=3.712(2)$ Å, $b=3.895(4)$ Å, and $c=11.685(4)$ Å, with $c/a=3.061$ and $(b-a)/(b+a)=9.98\times 10^{-3}$. These values indicate an oxygen deficiency $\delta\sim 0$.¹⁴ The powder sample was examined with an optical microscope, and the grains appeared to be well-formed single crystals with a roughly cubic shape with dimensions ~ 25 (μm)³; this was the sample used in our study of the superconducting fluctuation diamagnetism above T_c in YBa₂Cu₃O₇.³ Some of our $C(T)$ data-analysis results given below for the pellet sample are reproduced in Ref. 7 (sample No. 6).

The results of a differential-thermal-analysis (DTA) measurement on the powder sample in oxygen gas using a Perkin-Elmer 1700 DTA with a System 7/4 controller are shown in Fig. 1(a). The small endothermic peak with an onset near 925°C is the melting transition of the Ba- and Cu-rich Y-Ba-Cu-O eutectic composition impurity.¹⁵ In order to ascertain the amount of eutectic impurity present in the YBa₂Cu₃O₇ powder, a small powder sample consisting of 90 wt % powder YBa₂Cu₃O₇ was mixed with 5 wt % BaCuO₂ and 5 wt % CuO, and the mixture heated to 960°C in a tube furnace under O₂ gas to form a eutectic mixture plus YBa₂Cu₃O₇ majority phase. A DTA scan as in Fig. 1(a) was then performed, and the results are shown in Fig. 1(b). The ratio of the enthalpy under the peak in Fig. 1(a) to that in Fig. 1(b) is 0.060, which indicates that (0.6 ± 0.2) wt % of our YBa₂Cu₃O₇ powder sample consists of the eutectic impurity mixture. Since this consists of little Y₂O₃ and approximately equal amounts of CuO and BaCuO₂,¹⁵ our batch contains 0.3(1) wt % BaCuO₂.

Heat-capacity $C(T)$ measurements were carried out on the pellet sample of YBa₂Cu₃O₇ using pulse calorimeters at Ames (1.5–105 K, accuracy of 1–2 %) and at Berkeley (0.4–30 K, accuracy of $\approx 0.3\%$). Additional $C(T)$ measurements, accurate to 0.5%, were made on the pellet sample in Berkeley from 68 to 110 K using a high-resolution continuous-heating method, with a heating rate of ≈ 4 mK/s. The measurements at Berkeley were made in $H=0$ and 70 kG.

In the Ames pulse $C(T)$ measurements, a small amount of Apiezon N grease was used to attach the sample to a copper plate, with the thermometer attached to the opposite side of the plate. For the pulse $C(T)$ measurements at Berkeley, the sample was wrapped with silver foil to enhance the thermal contact between sample and addenda, and attached to a copper plate with a small amount of GE 7031 varnish. A small thin-film heater was mounted onto the silver foil. In these measurements, the duration of a heat pulse was about 2 min at 30 K and 30 s below ≈ 10 K. The thermal equilibration time was about 5 min at the lowest temperatures and 10 min near 30 K.

$C(T)$ data for both the powder and pellet samples were

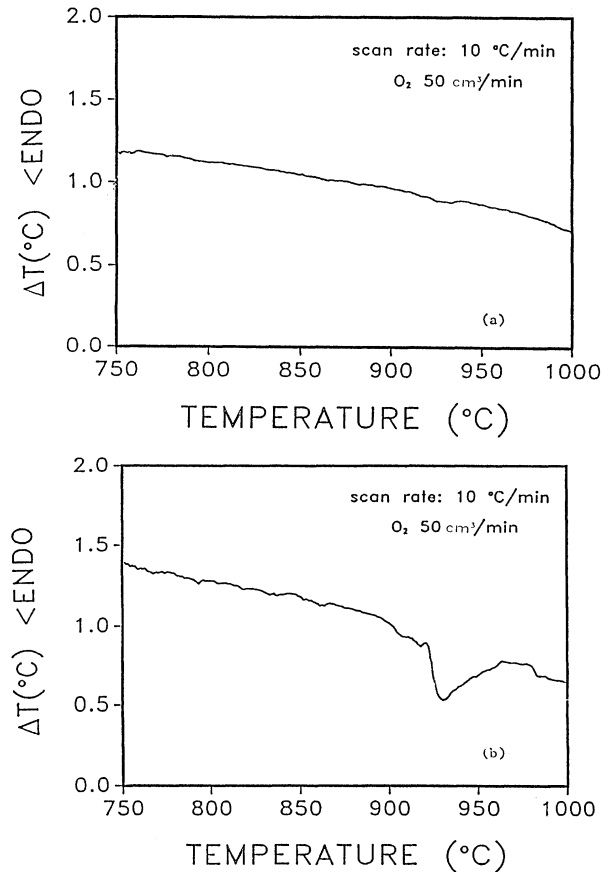


FIG. 1. Differential thermal analysis scans in O₂ gas for (a) our YBa₂Cu₃O₇ powder sample and (b) a mixture of 90 wt % of the powder sample with 5 wt % CuO and 5 wt % BaCuO₂.

obtained between 110 and 400 K using a Perkin-Elmer DSC 7 differential scanning calorimeter (DSC) at heating and cooling rates of 10°C/min in a search for possible phase transitions. The accuracy near 250 K is 1%, decreasing to 8% near 150 K.¹⁶

For comparison with the $C(T)$ data, magnetic susceptibility data for some of the same samples were obtained at Ames using a Quantum Design superconducting quantum interference device (SQUID) magnetometer.

The Ames pulse $C(T)$ measurements were made first on a single cooldown. Next, a series of measurements (runs *A*, *B*, and *C*) between 65 and 105 K were made at Berkeley. During these measurements, an unusual run-to-run irreproducibility was observed. The sample was then warmed to room temperature, recooled, remeasured between 65 and 110 K (run *D*), cooled to 0.4 K, and measured in $H=0$ and then in 70 kG, all at Berkeley. Finally, the Ames DSC measurements were made.

III. RESULTS

An overview of $C(T)$ of the YBa₂Cu₃O₇ pellet sample in zero applied magnetic field from 1.5 to 400 K is shown

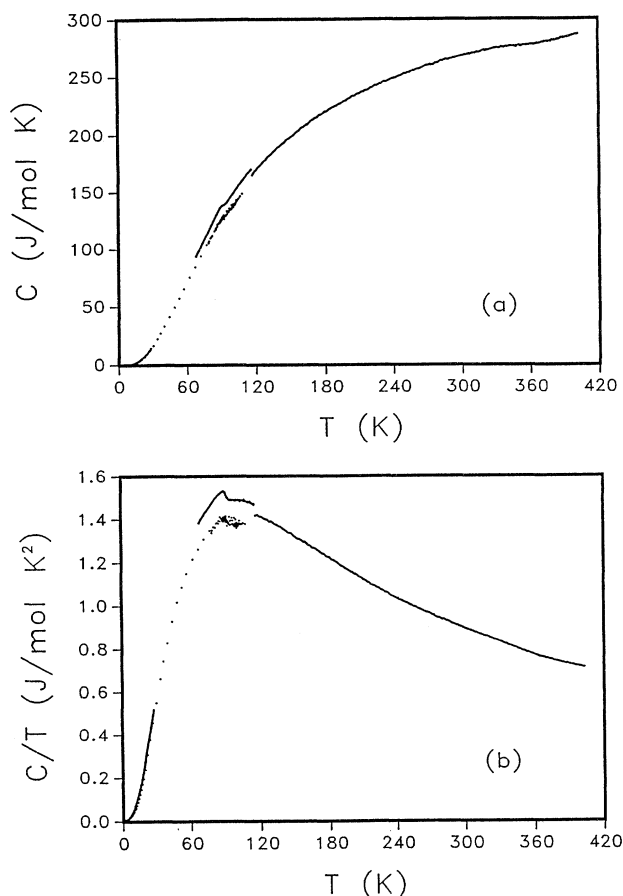


FIG. 2. (a) Overview of heat capacity C vs temperature T for a polycrystalline $\text{YBa}_2\text{Cu}_3\text{O}_7$ pellet sample in zero applied magnetic field from pulsed calorimeter measurements at Ames (< 110 K), pulsed calorimeter measurements at Berkeley (1–30 K), continuous-heating calorimeter measurements at Berkeley (68–110 K, top data set here, set A in Fig. 3), and differential scanning calorimeter measurements at Ames (110–400 K). (b) C/T -vs- T data derived from (a).

in Fig. 2(a) (C versus T) and Fig. 2(b) (C/T versus T). There are discrepancies, on the order of 5%, between the $C(T)$ near 110 K measured using the pulsed- and continuous-heating calorimeters and the DSC. The magnitude of the heat capacity over the whole temperature range is similar to the results of previous measurements on relatively magnetically pure samples.^{5,17}

A series of four measurements was carried out using the Berkeley continuous-heating calorimeter. Initially, the sample was cooled from room temperature to 65 K and held at that temperature overnight. Curve A in Fig. 3 shows the first measurement ($H=0$) up to ≈ 110 K. A feature with a peak near 89.5 K is clearly observed, associated with the onset of superconductivity. Following the usual procedure, the sample was then cooled again to 65 K, held overnight, and the measurement repeated (labeled B in Fig. 3). The temperature of the peak in C/T for B increased to 91.0 K from the value of 89.5 K found

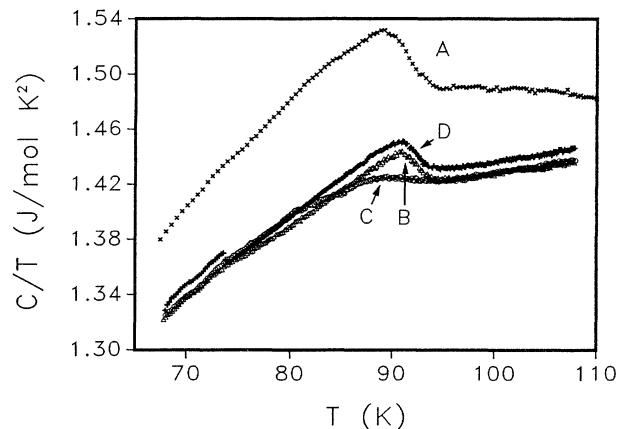


FIG. 3. Heat capacity divided by temperature C/T vs T for $T \sim T_c$ measured at Berkeley using a continuous-heating technique for the $\text{YBa}_2\text{Cu}_3\text{O}_7$ pellet sample. The sequence was as follows. A : cooled from room temperature and held overnight at 65 K in zero applied magnetic field H before measurement; B : cooled from 110 K and held at 65 K overnight ($H=0$); C : cooled from 110 K and held at 65 K overnight, then $H=70$ kG applied; D : cooled from room temperature ($H=0$) and held at 65 K overnight.

for A . From Fig. 3, large differences between the two measurements are seen in both the magnitude of $C(T)$ and the size of the feature near T_c . Also, there are hints of anomalies near 102 and 74 K in B not evident in A . There were no apparent differences in the manner in which the data sets A and B were accumulated and analyzed. There is no precedent for the change in behavior between runs A and B in measurements on $\text{YBa}_2\text{Cu}_3\text{O}_7$ at Berkeley.

Next, the sample was again cooled to 65 K and held overnight. A magnetic field of 70 kG was applied and $C(T)$ measured (curve C in Fig. 3) in the same manner as in the first two experiments. The feature at T_c is smeared out by the field as reported earlier,^{5,18} and the temperature of the maximum in C/T has decreased to 88.5 K. There is a clear crossover of the data sets B and C near 85 K. Near 65 K and above 95 K, the B and C data sets coincide, and both show evidence of a feature at 102 K. The relation between the data from runs B and C is typical of that observed in other samples, except for the relatively marked suppression of the peak in C/T in 70 kG, which is more typical of single-crystal data for $\mathbf{H}||c$, even though x-ray-diffraction measurements of the surface of the pellet indicated a random orientation of the grains (see below). After measurement C , the sample was warmed to room temperature, cooled to 65 K in zero field and held overnight, and a fourth data set obtained (set D in Fig. 3) using the same heating rate as before. Remarkably, the weak anomaly at 75 K in set B appears now as a sharp mean-field-like second-order transition in set D .

The results of the pulse $C(T)$ measurements in zero field from 0.5 to 10 K at Ames and Berkeley are shown in Fig. 4. Figure 5 shows the data obtained at Berkeley in

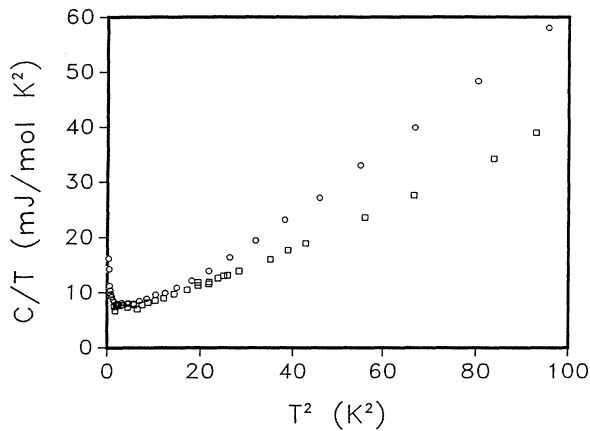


FIG. 4. Low-temperature pulsed heat capacity divided by temperature C/T vs T^2 in zero field measured at Ames (squares) and Berkeley (circles).

both zero field and 70 kG. The zero-field heat-capacity measurements show a clear upturn in C/T below about 2 K. In $H=70$ kG, a clear Schottky-like anomaly appears with a peak near 3 K; at very low T (<0.5 K), a sharp upturn in C/T is observed.

An expanded plot of the DSC data for the pellet sample of $\text{YBa}_2\text{Cu}_3\text{O}_7$ in Fig. 2(a) from 120 to 400 K taken with increasing T is shown in Fig. 6, where data for the same sample with decreasing T and for the powder sample with increasing T are also included. With increasing T , an anomaly near 330 K is seen for the pellet sample which is not obviously present in the measurement with decreasing T . From Fig. 6, there is no evidence of an anomaly near 220–240 K. There is also no evidence of any anomalies in $C(T)$ for the powder sample upon increasing or decreasing (not shown) the temperature.

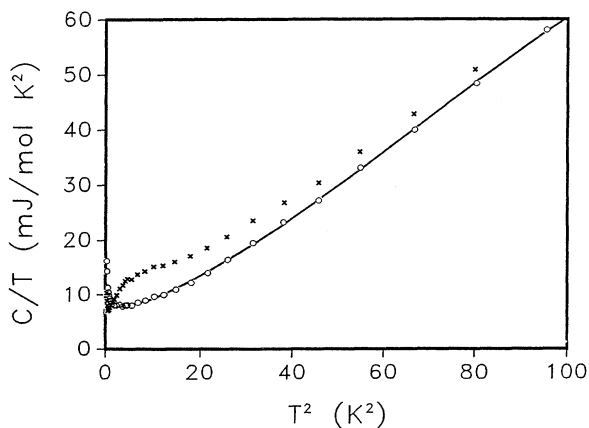


FIG. 5. Low-temperature pulsed heat capacity divided by temperature C/T vs T^2 measured at Berkeley with $H=0$ (circles) and 70 kG (crosses); the zero-field data are the same as in Fig. 4 from Berkeley. The solid curve is a fit to the zero-field data (see text).

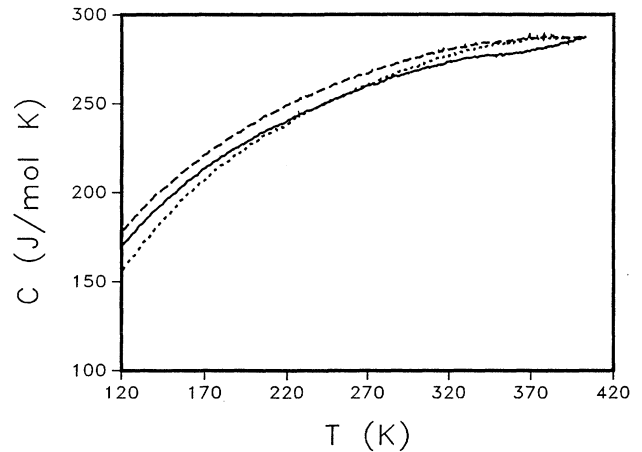


FIG. 6. Heat capacity C vs temperature T measured at Ames using a differential scanning calorimeter with a temperature scanning rate of $10^\circ\text{C}/\text{min}$. The solid data set was taken on heating the $\text{YBa}_2\text{Cu}_3\text{O}_7$ pellet sample, the long-dashed data on cooling the pellet sample, and the short-dashed data on heating the powder sample.

Magnetic susceptibility $\chi(T)$ data above T_c for the pellet and powder samples of $\text{YBa}_2\text{Cu}_3\text{O}_7$ in fields of 30 or 50 kG are shown in Fig. 7. The powder was aligned with the c axis parallel to the field using a method described previously,³ whereas the grains in the pellet were found using x-ray diffraction of the surface to be randomly aligned, presumably due to the approximately cubic morphology of the grains. The data for the pellet sample show a clear cusp at ≈ 320 K, whereas the data for the powder exhibit no evidence of an anomaly above T_c . Because of the proximity of the cusp temperature for the pellet to that of the heat-capacity anomaly observed above with the DSC on heating, the source of the

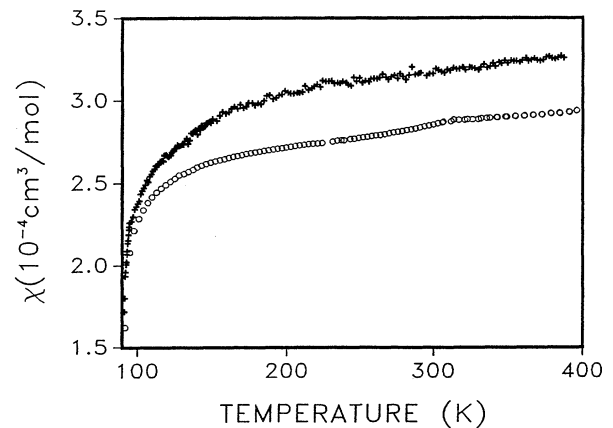


FIG. 7. Magnetic susceptibility χ vs temperature from 95 to 400 K for $\text{YBa}_2\text{Cu}_3\text{O}_7$. Open circles: 191-mg piece of the pellet sample with randomly oriented grains ($H=50$ kG); crosses: 17.6 mg of the powder sample with the grains aligned with $c||\mathbf{H}$ ($H=30$ kG).

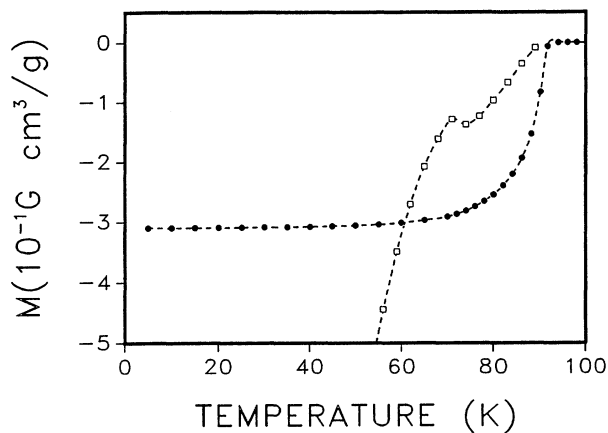


FIG. 8. Magnetization M vs temperature for a piece of the pellet sample of $\text{YBa}_2\text{Cu}_3\text{O}_7$ in applied fields of 50 G (solid circles) and 50 kG (open squares).

anomalies in the two types of measurement may be the same, but in any case is not yet understood.

Magnetization-versus-temperature $M(T)$ data below T_c for the pellet sample in fields of 50 G and 50 kG are shown in Fig. 8. The low-field data show a sharp superconducting onset at 91.8 K and a shielding fraction at 5

K of 127% uncorrected for demagnetization factors. The 50-kG data exhibit an anomaly near 75 K. This anomaly might be a manifestation of flux-pinning effects, although this appears unlikely because the magnetization is reversible with increasing and decreasing field at this field and temperature.¹⁹ Alternatively, it could be a reflection of some sort of phase transition occurring at this temperature as is suggested clearly in the zero-field $C(T)$ data set D for the pellet in Fig. 3—the $M(T)$ measurements were made after run D in which the 75-K feature in $C(T)$ was first observed. To investigate this question further, zero-field-cooled (ZFC) and field-cooled (FC) $M(T)$ data were obtained on heating with $H=3, 20, 30, 40,$ and 50 kG and are plotted in Fig. 9. Each data set with $H \geq 20$ kG shows evidence for an anomaly near 70 K. The anomaly is most pronounced at the higher fields, and the temperature T_0 at which the anomaly occurs on heating increases linearly with H at a rapid rate $dT_0/dH \approx 0.30$ K/kG for $20 \text{ kG} \leq H \leq 40 \text{ kG}$. For $H \leq 40$ kG, there is little or no observable difference between the ZFC and FC data over the plotted temperature ranges. If the anomalies in $C(T,0)$ and $M(T,H)$ are related to each other and arise from the same phase transition, as they appear to, the increase in T_0 with H is very unusual and is inconsistent with the behavior expected for a phase transition associated with the magnetic-flux lattice. At $H=50$ kG, the

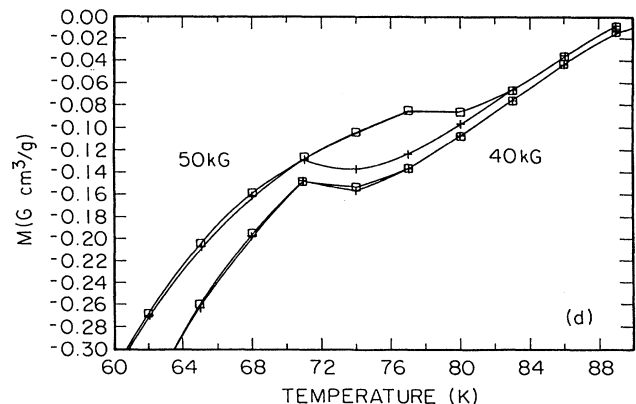
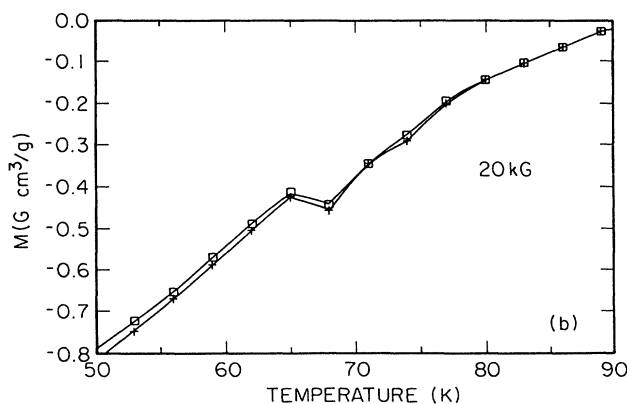
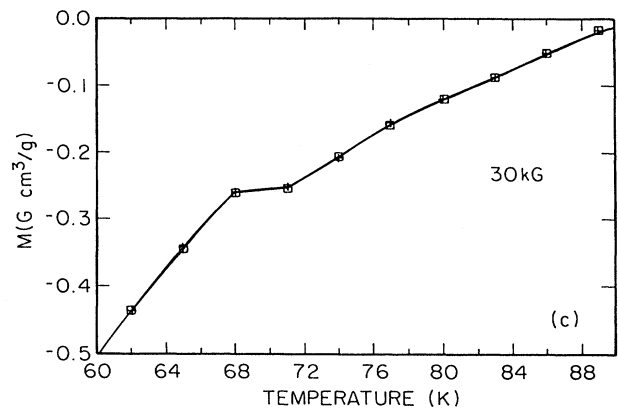
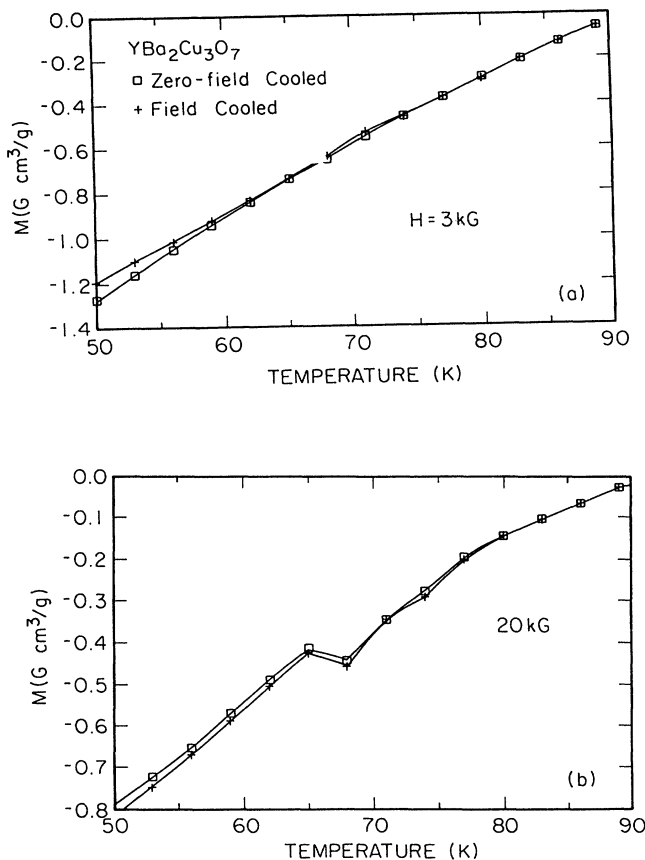


FIG. 9. Magnetization M vs temperature for the pellet sample of $\text{YBa}_2\text{Cu}_3\text{O}_7$, in applied magnetic fields of (a) 3 kG, (b) 20 kG, (c) 30 kG, and (d) 40 and 50 kG.

ZFC and FC data are different between 70 and 83 K, but coincide closely on either side of this range.

IV. ANALYSIS AND DISCUSSION

A. Heat capacity near T_c

Here we will discuss the results in Fig. 3 of the set of four sequential $C(T)$ measurements using the continuous-heating method at Berkeley. The differences between the first data set A in zero field and the subsequent zero-field sets B and D are striking. Near T_c , the heat capacity in B is about 6% less than in A . Using the traditional method of entropy balance to estimate the heat-capacity jump at T_c (but see below), one obtains $\Delta C/T_c = 32 \text{ mJ/K}^2 \text{ mol YBa}_2\text{Cu}_3\text{O}_7$ for B , which is 42% less than the value of 55 mJ/mol K^2 for A . This difference is much greater than the precision, and even the absolute accuracy, of each measurement. Thus it is real and must arise from a thermal history dependence of the heat capacity. Smaller differences are apparent between the data sets B and D . In D , a sharp anomaly at about 74 K is observed, which appears to be smeared out in set B and absent in set A ; this anomaly occurs at about the same temperature as that seen in the magnetization data for $H \geq 20 \text{ kG}$ in Fig. 9 and $H = 50 \text{ kG}$ in Fig. 8.

In an applied field of 70 kG, the heat capacity in a plot of C/T versus T (data set C) shows a smooth, broad peak at T_c and only a slight downward shift in the peak temperature compared with the zero-field data, as previously reported.^{5,18} As noted above, a sharp anomaly was observed at 74 K in data set D ; these data were taken in zero field after the high-field set C was obtained. Thus, although it seems unlikely, the magnetic-field history of the sample may be involved with the apparent irreproducibility of $C(T)$ in Fig. 3, in addition to the above influence of the thermal history. The C/T data set C in $H = 70 \text{ kG}$ is larger in magnitude than the zero-field set B between ≈ 75 and $\approx 85 \text{ K}$, whereas it is smaller between ≈ 85 and $\approx 93 \text{ K}$. In the latter region, the entropy change $\Delta S = S(0) - S(70 \text{ kG}) \approx 83 \text{ mJ/mol K}$, and in the former it is -55 mJ/mol K , yielding a net entropy change $\Delta S_{\text{net}} = 28 \text{ mJ/mol K}$. This apparent nonconservation of entropy could conceivably arise through the above thermal history dependence of $C(T)$ and/or from the limited temperature range of the measurements in Fig. 3.

Because of a lack of detailed knowledge of the dominant lattice contribution to the heat capacity of high- T_c cuprate superconductors near T_c , it is not clear how to accurately separate the observed heat capacity into electronic and lattice parts. A further complication is that close to T_c , the thermodynamic and electronic transport properties of the cuprate superconductors are dominated by the influence of superconducting fluctuations.⁴ Therefore, without taking into account the fluctuation term, one might infer an inaccurate mean-field heat-capacity jump ΔC at T_c , which would then lead to an inaccurate estimate of the normal-state Sommerfeld coefficient γ if one used, e.g., the BCS result relating γ to ΔC

($\Delta C/\gamma T_c = 1.43$).

We now consider the fluctuation contribution to be observed $C(T)$ to lowest order. After Refs. 3 and 4, we utilize a model in which there are two conducting layers per unit cell in $\text{YBa}_2\text{Cu}_3\text{O}_7$, each of which is assigned one complex s -wave order parameter; the layers are coupled by Josephson tunneling. Above T_c , the relationship between the superconducting fluctuation heat capacity $C_{\text{fl}}^+(T)$ and the superconducting fluctuation diamagnetism $\chi_c^{\text{fl}}(T)$ with $\mathbf{H} \parallel \mathbf{c}$ is given by⁴

$$C_{\text{fl}}^+(T) = -\frac{3\phi_0^2 \chi_c^{\text{fl}}(T)}{4\pi^2 T \xi_{ab}^4(0)} \propto -\chi_c^{\text{fl}}(T)/T, \quad (1)$$

where ϕ_0 is the flux quantum $hc/2e$ and $\xi_{ab}(0)$ is the zero-temperature Ginzburg-Landau coherence length within a CuO_2 layer. Below T_c in the three-dimensional fluctuation region, the fluctuation heat capacity $C_{\text{fl}}^-(T)$ is reduced from $C_{\text{fl}}^+(T)$ by $\sim \eta/\sqrt{2}$,^{8,20} where $\eta \leq 1$.

Using Eq. (1), the measured $\chi_c^{\text{fl}}(T)$, and the derived $\xi_{ab}(0)$, one can estimate the contributions $C_{\text{fl}}^+(T)$ and $C_{\text{fl}}^-(T)$ to the measured $C(T)$ above and below T_c , respectively. Then, by subtracting these contributions from $C(T)$, an estimate of the sum of the lattice and electronic heat capacities in the absence of superconducting fluctuations (mean-field heat capacity C_{MF}) can be obtained. Here we do not account for the superconducting transition width^{4,21} arising from chemical inhomogeneity in the sample. Therefore, the calculated fluctuation heat capacity diverges close to T_c (Fig. 10), in contrast to our observations. For temperatures somewhat removed from the average T_c , we expect the calculated fluctuation contributions to more accurately apply to the observations.

In Fig. 11(a), we replot the observed C/T -versus- T data set D in Fig. 3 (crosses) and $C_{\text{MF}}(T)$ derived as described above (open circles) for the temperature ranges 81–85 and 95–101 K, using $\xi_{ab}(0) = 13.6 \text{ \AA}$ and $\chi_c^{\text{fl}}(T)$ from Ref. 3. For the temperature region closer to T_c , we linearly extrapolated $C_{\text{MF}}(T)$ on both sides of T_c to T_c

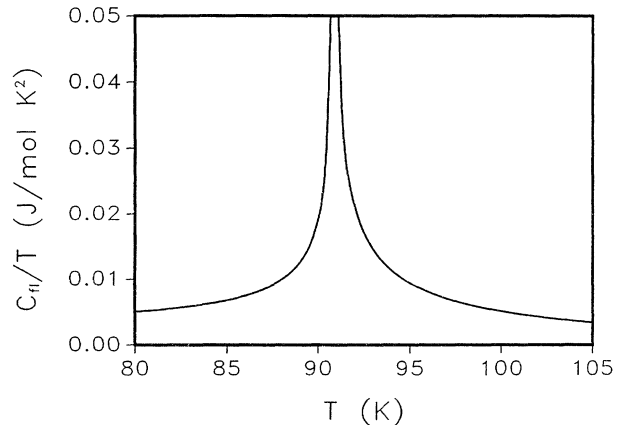


FIG. 10. Superconducting fluctuation heat capacity divided by temperature C_{fl}/T vs T , calculated using the data and parameters from Ref. 3 and the theory of Ref. 4.

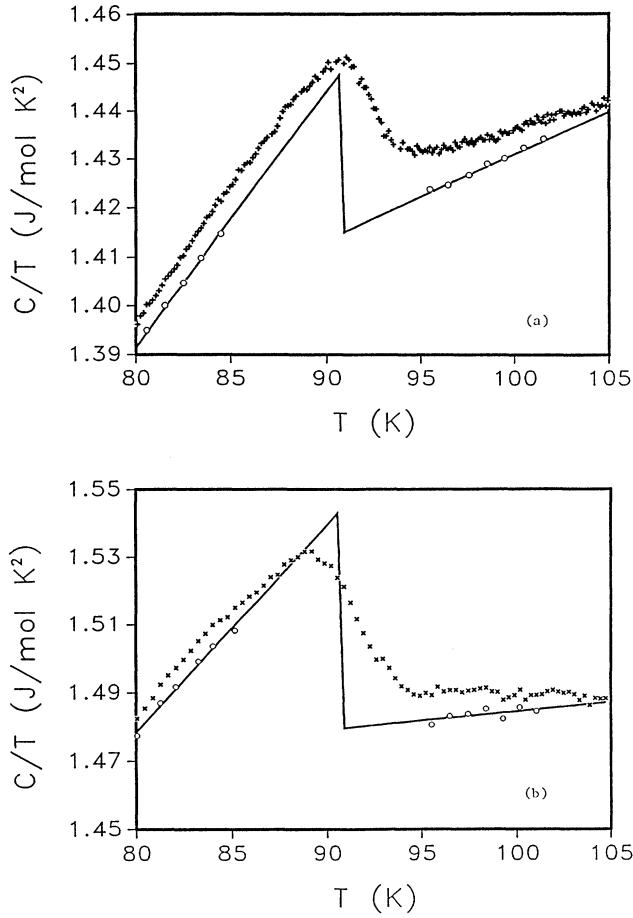


FIG. 11. (a) Observed heat capacity (plus symbols) from data set *D* in Fig. 3 compared with the sum of the estimated mean-field electronic and lattice heat capacities (solid lines). (b) Same as (a), but for data set *A* from Fig. 3.

(solid lines). T_c was taken to be 90.8 K, the temperature at which a pulsed $C(T)$ data set taken at Ames over a limited temperature range spanning T_c (not presented here) showed a sharp cusp. This is also the temperature at which the magnetization data for $H=50$ G in Fig. 8 showed a sharp onset and is the average peak temperature of $C(T)/T$ for data sets *A*, *B*, and *D* in Fig. 3. From Fig. 11(a), the mean-field heat-capacity jump at T_c is inferred to be $\Delta C_{MF}(T_c)/T_c \approx 33$ mJ/mol K², coincidentally nearly the same as the above value $\Delta C/T_c = 32$ mJ/mol K² obtained using conventional entropy balance near T_c . The value of ΔC_{MF} yields $\gamma_{MF} \approx 23$ mJ/mol K² using the above BCS weak-coupling mean-field result. This γ_{MF} value is less than most reported γ values.^{5,6,17} However, this value is consistent with the value (26 mJ/mol K²) obtained from a free-electron gas analysis of the spin susceptibility³ above T_c derived from $\chi(T)$ data as in Fig. 7. We estimate the density of states at the Fermi energy to be $D(E_F) = 3.3$ states/(eV Cu atom)⁻¹ using the relation $\gamma_{MF} = \pi^2 \mu_B^2 D(E_F)/3k_B$.

A similar analysis of the $C(T)$ data set *A* in Fig. 3 is shown in Fig. 11(b). Here we find $\Delta C_{MF}/T_c = 64$ mJ/mol K² and $\gamma_{MF} = 44$ mJ/mol K² in the BCS weak-coupling limit. The $\Delta C_{MF}/T_c$ value is somewhat larger than the above value $\Delta C/T_c = 55$ mJ/mol K² obtained using conventional entropy balance near T_c .

B. Heat capacity between 0.4 and 10 K

The Ames and Berkeley pulse calorimeter measurements are in agreement below ~ 5 K, as seen in Fig. 4. At higher temperatures, a large difference becomes apparent; both measurements are accurate to within 1–2% below 30 K, and so this difference is real. The source of this difference between the two $C(T)$ data sets above 5 K is not known. This difference amounts to a difference in the lattice heat capacity apparently induced by changes in the thermal and/or magnetic-field history of the sample, as documented near T_c in Fig. 3 and above 120 K in Fig. 6. The two $C(T)$ data sets in Fig. 4 yield Debye temperatures differing by more than 30 K (see below).

In Figs. 4 and 5, the low-temperature upturn in $C(T, H=0)/T$ starts near 2 K, arising primarily from magnetically isolated Cu²⁺ local magnetic moments. A common impurity in YBa₂Cu₃O₇ samples is BaCuO₂ (Refs. 22 and 23) and is one of the components of the eutectic impurity present in our samples as documented above. Some samples of BaCuO₂ exhibit $C(T)/T$ behavior nearly independent of T at low T , while others show an upturn.^{22,24} Considering the presence of this impurity phase as well as localized Cu²⁺ moments in the pellet sample of YBa₂Cu₃O₇, we fit the zero-field $C(T)$ data with the expression

$$C(T) = \frac{A_{-2}}{T^2} + \gamma^*(0)T + B_3 T^3 + B_5 T^5 + B_7 T^7, \quad (2)$$

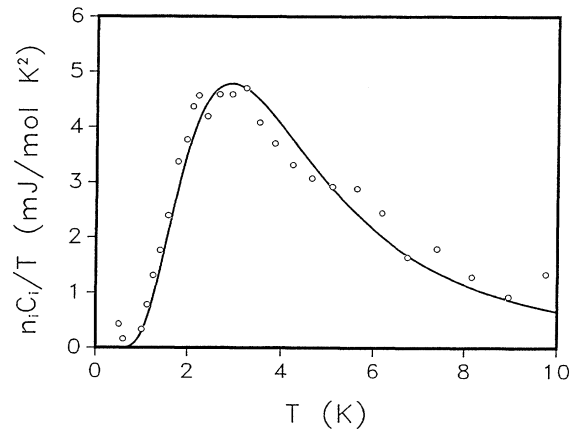


FIG. 12. Heat capacity of the magnetically isolated Cu²⁺ magnetic defects derived from the observed data divided by temperature $n_i C_i / T$ vs T for the YBa₂Cu₃O₇ pellet sample in a field of 70 kG (open circles). The solid curve is the theoretical prediction for $n_i = 0.0044$ mol of magnetically isolated spin- $\frac{1}{2}$ defects per mole of YBa₂Cu₃O₇.

where the first term accounts for the low- T upturn, the second is a linear term of unknown origin, and the remaining terms are due to the lattice contribution. Fitting Eq. (2) to the zero-field data in Fig. 5 yields $A_{-2}=13.1(3)$ mJ K/mol, $\gamma^*(0)=5.0(1)$ mJ/mol K², $B_3=0.33(1)$ mJ/mol K⁴, $B_5=4.22(8)\times 10^{-3}$ mJ/mol K⁶, and $B_7=2.02(4)\times 10^{-5}$ mJ/mol K⁸. From the value of B_3 , the calculated Debye temperature $\Theta_D=422(8)$ K, which is similar to reported values.^{5,25,26} For the Ames $C(T)$ data set in Fig. 4, $\gamma^*(0)=5.7(6)$ mJ/mol K², which is equal within experimental error with the value from the Berkeley data, whereas $\Theta_D=456$ K, about 30 K larger than the Berkeley value. The large difference between the Ames and Berkeley data sets between 5 and 10 K is real, as noted above, and apparently arises from the different thermal histories of the sample in the two measurements.

It is known that a sufficiently high magnetic field can cause the $C(T)/T$ upturn for $H=0$ to become a Schottky-like anomaly.²⁷ In Fig. 5, for $H=70$ kG, there is indeed a broad maximum in $C(T)/T$ near 3 K, and there is a sharp upturn at much lower temperature. This sharp upturn is from the coupling between the magnetic field and the Cu nuclear moments.^{27,28} To analyze the $H=70$ kG results, we used the expression

$$C(T) = \frac{A_{\text{hf}}}{T^2} + n_i C_{\text{Sch}}(T) + \gamma^*(H)T + C_{\text{lattice}}, \quad (3a)$$

with

$$C_{\text{Sch}}(T) = R \frac{\delta^2}{T^2} \frac{e^{\delta/T}}{(1+e^{\delta/T})^2}, \quad (3b)$$

where the first term in Eq. (3a) is due to the hyperfine interaction, the next term is the Schottky anomaly due to n_i mole fraction of isolated Cu^{2+} defects, $C_{\text{Sch}}(T)$ is the heat capacity per mole of these defects, and $\gamma^*(H)T$ is the linear contribution in the 70-kG magnetic field. In Eq. (3b), R is the molar gas constant and δ is the energy splitting in K of the spin- $\frac{1}{2}$ Zeeman levels in the field H : $\delta = g\mu_B H/k_B$, where we assume a gyromagnetic factor $g=2$. From a fit to the data on a CT^2 -versus- T^3 plot at low T , we find $A_{\text{hf}}=0.47(1)$ mJ K/mol $\text{YBa}_2\text{Cu}_3\text{O}_7$, which is close to the theoretical value of 0.50 mJ K/mol for the 3 mol of Cu, 2 mol of Ba, and 1 mol of Y nuclei in 1 mol of $\text{YBa}_2\text{Cu}_3\text{O}_7$.^{5,10,28} $\gamma^*(H=70$ kG) is found to be 6.5(2) mJ/mol K². From $\gamma^*(H=0)$ and $\gamma^*(H=70$ kG), we have $\partial\gamma^*/\partial H \approx 0.021$ mJ/mol K² kG, which is similar to the reported value.¹⁰ By subtracting the hyperfine, linear, and lattice (from the $H=0$ fit) terms from the observed $C(T, H=70$ kG) data according to Eq. (3a), the experimental isolated Cu^{2+} contribution to $C(T, H=70$ kG) was computed and is plotted versus T in Fig. 12 (open circles). Also shown is the theoretical Schottky contribution $n_i C_{\text{Sch}}(T)$ from Eq. (3b) for $n_i=0.0044$ (solid curve), where excellent agreement with the data is seen; this agreement illustrates the accuracy of the data and demonstrates the validity of Eqs. (3).

The impurity mole fraction due to isolated Cu^{2+} defects, n_i , was found above to be 0.0044(1) mol Cu^{2+} /mol $\text{YBa}_2\text{Cu}_3\text{O}_7$. This could arise from isolated defects in the $\text{YBa}_2\text{Cu}_3\text{O}_7$ majority-phase lattice itself and/or in the Ba-

CuO_2 impurity lattice. The latter possibility is consistent with the magnetic-field dependence of $C(T)$ for a BaCuO_{2+x} sample²⁹ that shows a low- T upturn in C/T . The above DTA measurements revealed the presence of 0.3(1) wt % BaCuO_2 impurity phase in our batch of $\text{YBa}_2\text{Cu}_3\text{O}_7$. If the upturn in the zero-field $C(T)$ and the Schottky-like anomaly in $C(T, H=70$ kG) are generated from all of the Cu^{2+} moments in this amount of BaCuO_2 , one would expect $n_i=0.014(5)$ mol Cu^{2+} /mol $\text{YBa}_2\text{Cu}_3\text{O}_7$, significantly greater than the observed n_i value. Thus the bulk of the Cu^{2+} ions in the BaCuO_2 impurity phase do not contribute to the zero-field low-temperature upturn in the observed $C(T)$.

The nonzero $\gamma^*(T=0, H=0) \equiv \gamma^*(0)$ value evidently arises from the $\text{YBa}_2\text{Cu}_3\text{O}_7$ phase and/or the bulk BaCuO_2 impurity phase [the contribution to $\gamma^*(0)$ from CuO impurity is negligible]. We consider first the second possibility. The above value of 0.3(1) wt % BaCuO_2 corresponds to $n_{\text{BCO}}=0.014(5)$ mol BaCuO_2 /mol $\text{YBa}_2\text{Cu}_3\text{O}_7$. For BaCuO_2 heat treated in a way similar to the preparation of our samples of $\text{YBa}_2\text{Cu}_3\text{O}_7$, one expects $\gamma_{\text{BCO}} < 80$ mJ/mol BaCuO_2 from published heat-capacity data.²² Thus we expect the impurity contribution γ_i to our measured $\gamma^*(0)$ for $\text{YBa}_2\text{Cu}_3\text{O}_7$ to be given by $\gamma_i = n_{\text{BCO}}\gamma_{\text{BCO}} < 1.1(4)$ mJ/mol $\text{YBa}_2\text{Cu}_3\text{O}_7$ K². This value is much less than the above observed values $\gamma^*(0)=5.0(1)$ and 5.7(6) mJ/mol K². We conclude that the $\gamma(0)$ associated with the $\text{YBa}_2\text{Cu}_3\text{O}_7$ phase in our pellet sample is $\gamma(0) \approx 4.0$ mJ/mol K². A similar value was obtained by Reeves *et al.*,³⁰ based on a Raman-scattering determination of the BaCuO_2 concentration, coupled with low-temperature $C(T)$ measurements.

The question now arises as to whether this $\gamma(0)$ is intrinsic to a perfectly ordered $\text{YBa}_2\text{Cu}_3\text{O}_7$ lattice, or whether it arises in some way from the presence of lattice disorder. One scenario presented recently is that lattice disorder and the presence of resultant localized Cu^{2+} magnetic moments produces normal (nonsuperconducting) regions in the sample, resulting in a nonzero $\gamma(0)$ and an upturn in the low-temperature zero-field $C(T)/T$ associated with those regions.⁷

An alternative explanation which could give rise to an intrinsic $\gamma(0) > 0$ for $\text{YBa}_2\text{Cu}_3\text{O}_7$ is as follows. The bulk Cu ions in the CuO_2 planes and Cu-O chains of the structure appear to be essentially localized Cu^{2+} ions with spin $\frac{1}{2}$.^{31,32} Elementary spin-wave theory predicts that spin waves on a one-dimensional chain of spins $\frac{1}{2}$, with nearest neighbors antiferromagnetically coupled with exchange energy $E_{ij} = JS_i \cdot S_j$, should exhibit a magnetic heat capacity $C_m(T)$ which is linear in temperature and given per mole of spins by

$$C_m(T) = (\pi R 2^{1/2}/3)(T/J) \\ = (12.31 \text{ J/mol K})(T/J), \quad (4)$$

where J is in units of K. If one assumes that spin waves propagate along the Cu-O chains (where the Cu ions are assumed to be spin- $\frac{1}{2}$ Cu^{2+} ions) of $\text{YBa}_2\text{Cu}_3\text{O}_7$, which contains one chain Cu atom/formula unit, then an intrinsic linear term would be expected in the $C(T)$, with a

magnitude of the observed order. For example, if $J \simeq 1500$ K as in the CuO_2 planes of the structure,³² Eq. (4) predicts that $\gamma_m(0) \sim 8$ mJ/mol $\text{YBa}_2\text{Cu}_3\text{O}_7 \text{ K}^2$; exact calculations on finite chains³³ yield a $\gamma_m(0)$ closer to our inferred $\gamma(0) \simeq 4$ mJ/mol K^2 , assuming the same value of J . This hypothesis would explain the lack⁵ of a linear term in the low-temperature $C(T)$ for the Bi- and Tl-based cuprate superconductors, since these structures do not contain Cu-O chains. The existence of the spin waves (and/or other types of magnetic excitations) in the Cu-O chains of $\text{YBa}_2\text{Cu}_3\text{O}_7$ necessary to this hypothesis can be tested, in principle, via inelastic neutron-scattering experiments on large single crystals of this compound.

C. Heat capacity above 120 K

Our $\chi(T)$ data for the pellet sample in Fig. 6 partially confirm previous $\chi(T)$ measurements^{12,13} that anomalies sometimes occur at ~ 240 K, ~ 330 K, or both. The data for this sample show only the anomaly near 330 K with no obvious anomaly near 240 K. Our $C(T)$ data for the pellet sample taken on warming show an anomaly at ~ 330 – 350 K, and therefore appear to confirm that the corresponding anomaly in $\chi(T)$ is a bulk effect and not due to impurity phases. However, the anomaly in the $C(T)$ data for the pellet sample was not unambiguously observed on cooling, possibly due to the above thermal history dependence of $C(T)$. $\chi(T)$ and $C(T)$ data for our powder sample taken on warming from 120 to 400 K and cooling from 400 to 120 K showed no anomalies.

V. CONCLUDING REMARKS

We have accomplished some of the goals of our heat-capacity $C(T)$ study of high-purity $\text{YBa}_2\text{Cu}_3\text{O}_7$ enumerated in Sec. I. From a determination of the Ba-CuO₂ magnetic-impurity-phase concentration in our batch of this compound from differential-thermal-analysis measurements, coupled with analysis of low (> 0.4 K) temperature $C(T)$ measurements in zero and 70-kG applied magnetic fields, we conclude that the linear Sommerfeld heat-capacity coefficient associated with the $\text{YBa}_2\text{Cu}_3\text{O}_7$ phase in our pellet sample is $\gamma(0) \simeq 4.0$ mJ/mol K^2 . The origin of this $\gamma(0)$ is not yet clear. One possibility which has been considered is that this $\gamma(0)$ is an indication that part of the sample does not become superconducting; i.e., $\gamma(0)/\gamma$ is the normal fraction, where γ is the normal-state Sommerfeld coefficient.^{5,7,34} We suggest that some fraction (unknown as yet) of $\gamma(0)$ could also arise from thermal excitation of spin waves (and/or possibly from other magnetic excitations) on the Cu-O chains and could therefore be intrinsic to an atomically ordered $\text{YBa}_2\text{Cu}_3\text{O}_7$ structure. We hope that this hypothesis will be tested using inelastic neutron-scattering measurements on large single crystals.

It is clear by now that superconducting fluctuations have a dramatic influence on the thermodynamic and electronic transport properties of the high- T_c cuprates in the vicinity of T_c .^{3,4,8–11,18,35} Heat-capacity measurements on single crystals of $\text{YBa}_2\text{Cu}_3\text{O}_7$ near T_c show strong evidence for a non-mean-field shape, attributed to

these fluctuations.^{8,18} However, even a slight broadening of the superconducting transition, as in most polycrystalline samples of $\text{YBa}_2\text{Cu}_3\text{O}_7$, rapidly smooths out this shape to appear mean field like.²¹ Indeed, a mean-field-like shape was found for our pellet sample. Utilizing the data and theory in Refs. 3 and 4, a quantitative estimate of the fluctuation heat capacity was made and found to be significant on the scale of the measurements in Fig. 3. A lowest-order attempt was made to extract the mean-field heat capacity in the absence of the fluctuations. We find that the heat-capacity jump at T_c , deduced from $C(T)$ data using the conventional entropy balance technique, may be appreciably affected by the presence of the fluctuations.

There have been numerous reports in the literature of anomalies occurring at various temperatures in various measurements of $\text{YBa}_2\text{Cu}_3\text{O}_7$ which have not been confirmed as magnetic or structural transitions by neutron- or x-ray-diffraction techniques.^{12,13,26,36} We presented calorimetric evidence that one such anomaly in the magnetic susceptibility $\chi(T)$ at ~ 310 – 330 K (Ref. 12) is a bulk phase transition of some kind. The occurrence of these transitions is highly sample dependent, and it is not known what characteristics of the samples control their occurrence.^{12,26} In our experiments, for example, we found that the powder sample of $\text{YBa}_2\text{Cu}_3\text{O}_7$ did not show the anomalies at ~ 330 K in $C(T)$ and $\chi(T)$ seen for the pellet sample. Other powder samples, however, do show these anomalies.¹²

A sharp second-order anomaly at $T_0 \simeq 74$ K for the pellet sample is observed in both $C(T,0)$ and $M(T,H)$ data. We find that T_0 increases with H at a rate $dT_0/dH \simeq 0.30$ K/kG between 20 and 40 kG from the $M(T)$ data. An anomaly in the temperature dependence of the electrical noise amplitude in a thin film of $\text{YBa}_2\text{Cu}_3\text{O}_7$ ($T_c = 85$ K) was observed near 75 K.³⁷ An anomaly in $C(T)$ at 76 ± 4 K was reported for a nonsuperconducting sample $\text{YBa}_2\text{Cu}_3\text{O}_{\simeq 6.4}$.³⁸ In our case, the second-order transition at T_0 on cooling could conceivably be a transition from an s -wave state to a state containing an additional triple-order parameter,³⁹ a similar double peak in $C(T)$ was recently observed below T_c for the heavy-fermion superconductor UPt_3 .⁴⁰

Finally, and unexpectedly, our $C(T)$ measurements on the pellet sample of $\text{YBa}_2\text{Cu}_3\text{O}_7$ revealed a surprisingly strong influence of the thermal and/or magnetic-field history of the sample. The magnitudes of $C(T)$ in both the low- (5–10 K) and higher- (70–120 K) T regimes were strongly influenced by the thermal and/or magnetic-field history. The heat-capacity jump at T_c and Debye temperature [but not the $\gamma^*(0)$ value] derived from these data were quite different for different experiments, and the shape and size of the 74-K anomaly were also strongly history dependent. These types of effects have been observed in elastic measurements of various types, where it is found that such effects are highly sample dependent.²⁶ Thus, for example, the heat capacities of most samples of $\text{YBa}_2\text{Cu}_3\text{O}_7$ near T_c are highly stable with time and thermal cycling, as found at Berkeley and elsewhere.³⁴ There is precedent for sample- and thermal-history-dependent transitions in the conventional lower- T_c ma-

terials. For example, the martensitic phase transitions observed calorimetrically in Nb₃Sn ($T_c = 18$ K) and V₃Si ($T_c = 17$ K) exhibit such dependences.^{41,42}

ACKNOWLEDGMENTS

The Ames group thanks A. Bevolo for use of his optical microscope, R. W. McCallum for extensive discussions of the Y₂O₃-CuO-BaO phase diagram and assistance with the DTA measurements, and C. A. Swensen

for assistance with the Ames pulse heat-capacity measurements. Ames Laboratory is operated for the U.S. Department of Energy by Iowa State University under Contract No. W-7405-Eng-82. The work at Ames was supported by the Director for Energy Research, Office of Basic Energy Sciences. The work at Berkeley was supported by the Director, Office of Energy Research, Office of Basic Energy Sciences, Material Sciences Division of the U.S. Department of Energy under Contract No. DE-AC03-76SF00098.

- *Present address: Department of Physics, University of Illinois at Urbana-Champaign, 1110 West Green Street, Urbana, IL 61801.
- †Present address: Materials Sciences Division, Bldg. 223, Argonne National Laboratory, Argonne, IL 60439.
- ¹Proceedings of the International Conference on High Temperature Superconductors and Materials and Mechanisms of Superconductivity, Interlaken, Switzerland, 1988 [Physica C **153-155** (1988)].
 - ²Proceedings of the International Conference on High Temperature Superconductors and Materials and Mechanisms of Superconductivity II, Stanford, CA, 1989 [Physica C **162-164** (1989)].
 - ³W. C. Lee, R. A. Klemm, and D. C. Johnston, Phys. Rev. Lett. **63**, 1012 (1989); W. C. Lee and D. C. Johnston, Phys. Rev. B **41**, 1904 (1990).
 - ⁴R. A. Klemm, Phys. Rev. B **41**, 2074 (1990).
 - ⁵For a review, see R. A. Fisher, J. E. Gordon, and N. E. Phillips, J. Supercond. **1**, 231 (1988).
 - ⁶For a review, see S. E. Stupp and D. M. Ginsberg, Physica C **158**, 299 (1989).
 - ⁷Norman E. Phillips, R. A. Fisher, J. E. Gordon, and S. Kim, Ref. 2, p. 1651; Norman E. Phillips, R. A. Fisher, J. E. Gordon, S. Kim, A. M. Stacy, M. K. Crawford, and E. M. McCarron III, Phys. Rev. Lett. **65**, 357 (1990).
 - ⁸S. E. Inderhees, M. B. Salamon, N. Goldenfeld, J. P. Rice, B. G. Pazol, and D. M. Ginsberg, Phys. Rev. Lett. **60**, 1178 (1988); **60**, 2445E (1988).
 - ⁹T. Laegreid, P. Tuset, O.-M. Nes, M. Slaski, and K. Fosshiem, Ref. 2, p. 490.
 - ¹⁰R. A. Fisher, J. E. Gordon, S. Kim, N. E. Phillips, and A. M. Stacy, Ref. 1, p. 1092.
 - ¹¹J. E. Gordon, M. L. Tan, R. A. Fisher, and N. E. Phillips, Solid State Commun. **69**, 625 (1989); Ref. 2, p. 484.
 - ¹²D. C. Johnston, S. K. Sinha, A. J. Jacobson, and J. M. Newsam, Ref. 1, p. 572; (unpublished).
 - ¹³M. Miljak, G. Collin, and A. Hamzic, J. Magn. Magn. Mater. **76-77**, 609 (1988); M. Miljak, G. Collin, A. Hamzic, and V. Zlatic, Europhys. Lett. **9**, 723 (1989).
 - ¹⁴D. C. Johnston, A. J. Jacobson, J. M. Newsam, J. T. Lewandowski, D. P. Goshorn, D. Xie, and W. B. Yelon, Am. Chem. Soc. Symp. Ser. **351**, 136 (1987).
 - ¹⁵R. W. McCallum, J. Met. **41**, 50 (1989); (private communication).
 - ¹⁶K. Sun, J. H. Cho, F. C. Chou, W. C. Lee, L. L. Miller, D. C. Johnston, Y. Hidaka, and T. Murakami, Phys. Rev. B (to be published).
 - ¹⁷A. Junod, D. Eckert, G. Triscone, V. Y. Lee, and J. Muller, Physica C **159**, 215 (1989).
 - ¹⁸M. B. Salamon, S. E. Inderhees, J. P. Rice, B. G. Pazol, D. M. Ginsberg, and N. Goldenfeld, Phys. Rev. B **38**, 885 (1988).
 - ¹⁹Sreeparna Mitra, J. H. Cho, W. C. Lee, D. C. Johnston, and V. G. Kogan, Phys. Rev. B **40**, 2674 (1989).
 - ²⁰P. Muzikar, Phys. Rev. Lett. **61**, 479 (1988); H. R. Brand and M. M. Doria, *ibid.* **61**, 480 (1988); S. E. Inderhees, M. B. Salamon, N. Goldenfeld, J. P. Rice, B. G. Pazol, D. M. Ginsberg, J. Z. Liu, and G. W. Crabtree, *ibid.* **61**, 481 (1988).
 - ²¹F. Sharifi, J. Giapintzakis, D. M. Ginsberg, and D. J. Van Harlingen, Physica C **161**, 555 (1989).
 - ²²R. Kuentzler, Y. Dossmann, S. Vilminot, and S. El Hadigui, Solid State Commun. **65**, 1529 (1988).
 - ²³S. Eriksson, L. G. Johansson, L. Börjesson, and M. Kakihana, Ref. 2, p. 59.
 - ²⁴D. Eckert, A. Junod, T. Graf, and J. Muller, Ref. 1, p. 1038.
 - ²⁵S. von Molnar, A. Torressen, D. Kaiser, F. Holtzberg, and T. Penny, Phys. Rev. B **37**, 3762 (1988).
 - ²⁶C. A. Swenson, R. W. McCallum, and K. No, Phys. Rev. B **40**, 8861 (1989).
 - ²⁷N. E. Phillips, R. A. Fisher, S. E. Lacy, C. Marcenat, J. A. Olsen, W. K. Ham, A. M. Stacy, J. E. Gordon, and M. L. Tan, Physica B **148**, 360 (1987).
 - ²⁸O. V. Lounasmaa, Phys. Rev. **128**, 1136 (1962).
 - ²⁹R. Ahrens, T. Wolf, H. Wohl, H. Rietschel, H. Schmidt, and F. Steglich, Ref. 1, p. 1008.
 - ³⁰M. E. Reeves, S. E. Stupp, T. A. Friedmann, F. Slakey, D. M. Ginsberg, and M. V. Klein, Phys. Rev. B **40**, 4573 (1989).
 - ³¹M. Horvatic, P. Segransan, C. Berthier, Y. Berthier, P. Budaud, J. Y. Henry, M. Couach, and J. P. Chaminade, Phys. Rev. B **39**, 7332 (1989).
 - ³²C. H. Pennington, D. J. Durand, C. P. Slichter, J. P. Rice, E. D. Bukowski, and D. M. Ginsberg, Phys. Rev. B **39**, 274 (1989).
 - ³³J. C. Bonner and M. E. Fisher, Phys. Rev. A **135**, 640 (1964).
 - ³⁴A. Junod, D. Eckert, T. Graf, G. Triscone, and J. Muller, Ref. 2, p. 842.
 - ³⁵See references cited in Refs. 3, 4, 8–11, and 18.
 - ³⁶See, e.g., S. Bhattacharya, M. J. Higgins, D. C. Johnston, A. J. Jacobson, J. P. Stokes, J. T. Lewandowski, and D. P. Goshorn, Phys. Rev. B **37**, 5901 (1988), and references therein.
 - ³⁷M. J. Ferrari, M. Johnson, F. C. Wellstood, J. Clarke, D. Mitzi, P. A. Rosenthal, C. B. Eom, T. H. Geballe, A. Kapitulnik, and M. R. Beasley, Phys. Rev. Lett. **64**, 72 (1990).
 - ³⁸E. Braun, H. Jackel, B. Roden, J. G. Sereni, and D. Wohlleben, Z. Phys. B **72**, 169 (1988).
 - ³⁹R. A. Klemm and S. H. Liu (unpublished).
 - ⁴⁰R. A. Fisher, S. Kim, B. W. Woodfield, N. E. Phillips, L. Taillefer, K. Hasselbach, J. Flouquet, A. L. Giorgi, and J. L. Smith, Phys. Rev. Lett. **62**, 1411 (1989).
 - ⁴¹R. Viswanathan and D. C. Johnston, Mater. Res. Bull. **8**, 589 (1971); Phys. Rev. B **13**, 2877 (1976).
 - ⁴²R. N. Shelton, D. C. Johnston, and R. Viswanathan, Mater. Res. Bull. **12**, 133 (1977).